Tropical Journal of Pharmaceutical Research February 2023; 22 (2): 271-276
ISSN: 1596-5996 (print); 1596-9827 (electronic)

Available online at http://www.tjpr.org
http://dx.doi.org/10.4314/tjpr.v22i2.7

Original Research Article

NR4A1 alleviates the toxicity in neural stem cells induced by propofol in early life by regulating AMPK pathway

Miaomiao Zhu, Jing Hu*, Baofeng Gao, Changlin Liu, Huiqing Li, Zengzhen Zhang

Department of Anesthesiology, Shandong Provincial Third Hospital, Jinan, Shandong Province 250031, China

For correspondence:* ***Email:* *jhu4376@163.com;* ***Tel:*** *+86-0531-81656166*

Sent for review: 31 October 2022 *Revised accepted: 31 January 2023*

Abstract

Purpose: *To examine the association of propofol (PRO) with related key genes that may serve as potential biomarkers for alleviation of PRO-induced toxicity in neural stem cells (NSCs).*
Methods: *Differentially expressed genes (DEGs) were screened based on GEO database, using the analysis platform of Metaboanalyst, GEO2R, DAVID and Ehbio. NSCs were purchased and treated with 3 μM of propofol (PRO). NR4A1 was transfected into NSCs, and the NR4A1 expression, apoptosis-related protein and AMPK pathway-related protein were determined by quantitative reverse transcription-polymerase chain reaction (qRT-PCR) and western blotting. Cell viability and apoptosis were evaluated by methylthiazolyldiphenyl-tetrazolium bromid (MTT) assay and flow cytometry.*
Results: *A total of 278 DEGs were analyzed on GSE106799 microarray, and finally screened for differentially expressed down-regulated gene, NR4A1, which is a hubgene. NR4A1 expression decreased in PRO-induced NSCs. Furthermore, NR4A1 attenuated the PRO-induced decrease in the viability of NSCs and the increase in apoptosis. Moreover, NR4A1 increased p-AMPK/AMPK level.*
Conclusion: *NR4A1 attenuates the toxicity in NSCs induced by PRO by regulating AMPK pathways, and thus provides a theoretical basis for the treatment of nerve damage caused by anesthetics.*

Keywords: *NR4A1, Eural stem cells, AMPK, Propofol, Hubgene*

Tropical Journal of Pharmaceutical Research is indexed by Science Citation Index (SciSearch), Scopus, Web of Science, Chemical Abstracts, Embase, Index Copernicus, EBSCO, African Index Medicus, JournalSeek, Journal Citation Reports/Science Edition, Directory of Open Access Journals (DOAJ), African Journal Online, Bioline International, Open-J-Gate and Pharmacy Abstracts

INTRODUCTION

Anesthetic management in the early stages of life is evidence of an association with neurodevelopmental disorders [1]. Commonly used anesthetic drugs, such as γ-aminobutyric acid agonists and N-methyl-D-aspartate antagonists, have varying degrees of neurotoxic effects on the developing brain, leading to neuronal apoptosis and as well as production of distant neuro behavioral deficits and cognitive impairment [2].

Early animal experiments have confirmed the adverse neurotoxic effects of general anesthetic drugs such as ketamine, N_2O, isoflurane and isoproterenol, which can produce extensive apoptotic degeneration of neurons, altered dendritic spine morphology, and impaired synaptic function in different species [3]. Therefore, it is important to study the

mechanisms of the effects of anesthetics on neurodevelopment.

Propofol (PRO) is the most frequently used short-acting intravenous anesthetic in clinical practice [4]. Because of the advantages of rapid induction, fast action, and short duration, PRO is widely used not only for induction of anesthesia but also for prolonged intraoperative anesthesia maintenance and postoperative intensive care unit (ICU) sedation [4]. It has been reported that PRO as a general intravenous anesthetic drug can induce neuronal apoptosis, and large doses and multiple exposures can impair cognitive function [5,6]. Moreover, PRO inhibits the self-renewal and differentiation of neural stem cells (NSCs), which precisely control brain development through self-renewal and differentiation [7]. Therefore, the search for potential biomarkers is highly important to mitigate the neurological damage caused by PRO.

Currently, among high-throughput experimental methods such as microarray analysis have been widely used for differentially expressed gene analysis [8]. A large amount of microarray data is stored in public databases. These repositories help researchers identify disease-associated biomarkers by integrating multiple microarray datasets. Gene Expression Omnibus (GEO) database is an international public database of high-throughput gene expression data, including sequencing and other forms of high-throughput functional genomic data, submitted by research institutions around the world.

Therefore, the aim of this study was to identify differentially expressed genes (DEGs) in PRO-treated and normal controls in order to find key down-regulated genes associated with PRO and to explore their mechanism of action.

METHODS

DEGs screening and correlation analysis

The gene expression dataset GSE106799 was downloaded from the GEO database (https://www.ncbi.nlm.nih.gov/geo/). The dataset consisted of four PRO samples (7-day old mice were injected with 50 mg/kg propofol) and four control samples (7-day old mice were injected with 50 mg/kg intralipid vehicle). The samples were normalized in line with the data, and then partial least squares regression analysis (PLSDA) was performed on the normalized genes through the metaboanalyst (https://www.metaboanalyst.ca/) analysis platform.

The GEO2R analysis platform (https://www.ncbi.nlm.nih.gov/geo/geo2r/) was used to compare two sets of samples to identify DEGs, and the DEGs were visualized with volcano plots to screen for up- and down-regulated DEGs. The screening criteria were $p < 0.01$ and fold change (FC) >1.5.

The screened DEGs were subjected to correlation analysis and heatmap analysis by metaboanalyst analysis platform.

KEGG enrichment analysis of DEGs

The DAVID (https://www.metaboanalyst.ca/) analysis platform was used to provide a comprehensive biofunctional annotation information for large-scale genes or proteins. KEGG pathway enrichment analysis of down-regulated DEGs genes was performed by the DAVID analysis platform, and bubble plots were made using the Ehbio (http://www.ehbio.com/ImageGP/) platform. $P < 0.05$ was considered statistically significant.

STRING (https://string-db.org/) was used to search for known proteins and predict protein-protein interactions (PPI). PPI analysis of down-regulated DEGs genes was performed using the STRING platform. Results were analyzed and visualized with Cytoscape software and screened for hubgene.

Cell treatment

Neural stem cells (NSCs) were purchased from LMAI Bio (Shanghai, China) and treated with 3 μM of PRO. NR4A1 and its negative control (NC) were transfected into NSCs.

Quantitative reverse transcription polymerase chain reaction (qRT-PCR)

RNA was extracted from NSCs using an RNA extraction kit (KeyGen Biotech, Nanjing, China), and reverse transcribed into cDNA; qRT-PCR was performed to analyze inflammatory factor mRNA expression levels using the Maxima SYBR Green Real-time PCR kit (KeyGen Biotech). β-Actin was used as an internal reference to calculate NR4A1 expression using the $2^{-\triangle\triangle Ct}$ method [9].

Western blotting (WB)

The total protein was extracted from NSCs by a protein lysis buffer (TaKaRa, Dalian, China), separated by SDS-PAGE and then transferred onto polyvinylidene fluoride (PVDF) membranes via electrophoresis. The proteins were incubated

with primary antibodies NR4A1 (1:1000, ab153914, Abcam, USA), Bax (ab182733), Bcl-2 (32124), cleaved Caspase 3 (ab49822), β-actin (ab179467), p-AMPK (ab92701) and AMPK (ab79885), and then incubated with horseradish peroxidase (HP)-labeled secondary antibody (1:1500, ab191866, Abcam). The incubated proteins were then rinsed in the blocking solution, developed in color development reagent, and imaged in gel imaging system.

Determination of cell viability

Methylthiazolyldiphenyl-tetrazolium bromid (MTT) assay were performed to determine cell viability. NSCs were added with MTT solution (10 mg/mL, Beyotime, Shanghai, China) to incubate for 4 h, and then added with dimethyl sulfoxide (DMSO) to shock for 10 min. The absorbance of 450 nm was measured by the spectrophotometer (Laspec, China).

Assessment of apoptosis

NSCs were stained by Hoechst Staining Kit (Beyotime), digested with 0.25% trypsin (Beyotime), added with Annexin-V and Propidium solution (Beyotime), and incubated for 20 min. The apoptosis ratio was determined by a flow cytometry (Beckman Coulter, USA). The results were expressed as the sum of early and late apoptotic rate.

Statistical analysis

The results of the experiments were analyzed by SPSS 22.0 software (SPSS Inc., USA) and displayed as mean ± standard deviation (SD). Analysis of variance (ANOVA) was used with Bonferroni test. The results were considered statistically significant at $p < 0.05$.

RESULTS

DEGs analysis outcome

In this section, the GSE106799 chip data was analyzed using GEO's GEO2R analysis platform. The normalization results of the data obtained from GSE106799 are shown in Figure 1 A. The results of PLSDA analysis of the normalized genes are shown in Figure 1 B, which show that the two samples were well distinguished from each other. A total of 278 DEGs were obtained from GSE106799, of which a total of 128 up-regulated differential genes and 150 down-regulated differential genes are shown in Figure 1 C. The heatmap of Figure 1 D and E also showed that the two different samples of the dataset are well distinguished from each other macroscopically.

The KEGG pathway analysis (Figure 1 F) showed that DEGs were mainly enriched in neuromodulation-related pathways. Cytoscape showed that NR4A1 was the centrally located hubgene as shown in Figure 1 G. The qRT-PCR results in Figure 1 H showed that NR4A1 expression was clearly down-regulated in PRO group ($p < 0.001$). Thus, NR4A1 was the differential gene associated with PRO treatment, and was most significantly down-regulated.

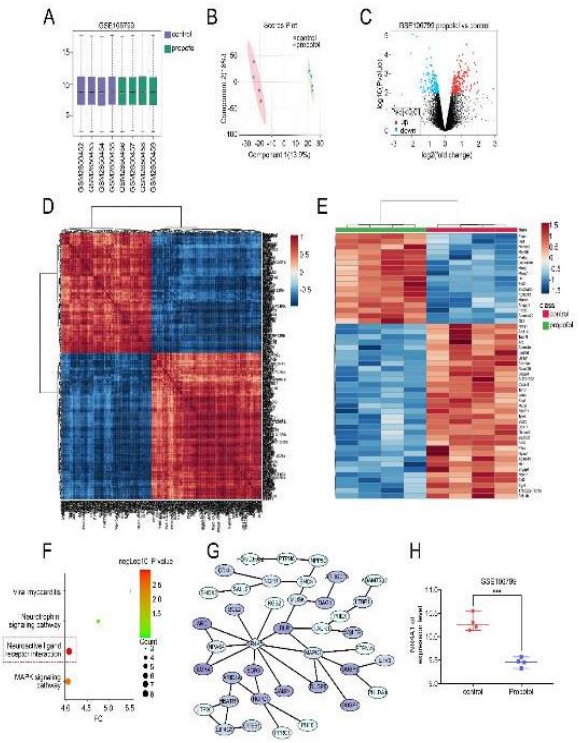

Figure 1: Search for differential genes based on GEO database (GSE106799). (A): The normalization results of the data obtained from GSE106799; (B): The results of PLSDA analysis; (C): Volcano plots of PRO samples and control samples. The red and blue dot distributions represent up- and down-regulated differential genes; (D and E): The headmap of PRO samples and control samples; (F): KEGG enrichment bubble diagram of DEGs; (G): The PPI network of DEGs; (H): Expression of NR4A1 was determined by qRT-PCR. ***$P < 0.001$

NR4A1 regulated cell motility in PRO-induced NSCs by affecting AMPK pathway

The effect of NR4A1 on NSCs induced by PRO was analyzed by RT-qPCR, WB, MTT assay and flow cytometry. Figure 2 A and B shows that PRO decreased mRNA and protein NR4A1 expressions compared with control group ($p < 0.001$).

In Figure 3 A, NR4A1 expression in PRO + NR4A1 group was higher than that in PRO + NC group, indicating that NR4A1 transfection succeeded. MTT assay results in Figure 3 B shows that PRO decreased cell viability, but NR4A1 alleviated the reduction of cell viability induced by PRO ($p < 0.05$). On the contrary, PRO significantly increased apoptosis, while NR4A1 clearly inhibited apoptosis in NSCs ($p < 0.05$). Moreover, the expressions of Bax and cleaved Caspase 3 were up-regulated, while Bcl-2 expression decreased, stimulated by PRO. However, the addition of Bax and cleaved Caspase 3, as well as the decrease in Bcl-2 were relieved when NR4A1 transfected into NSCs ($p < 0.05$). Finally, Figure 4 shows that PRO down-regulated p-AMPK/AMPK levels, but NR4A1 recovered restored p-AMPK/AMPK expression. Hence, these data demonstrated that NR4A1 enhanced the viability of NSC, but inhibited apoptosis induced by PRO through the regulation of AMPK pathway.

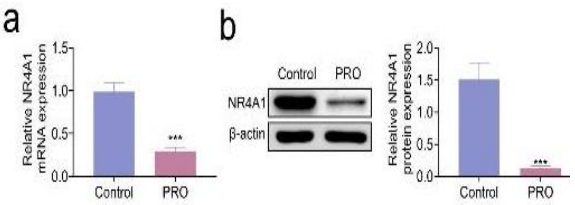

Figure 2: NR4A1 expression was down-regulated in NSCs. (A): Expression of NR4A1 was determined by RT-qPCR. (B): Expression of NR4A1 was determined by western blotting. ***$P < 0.001$

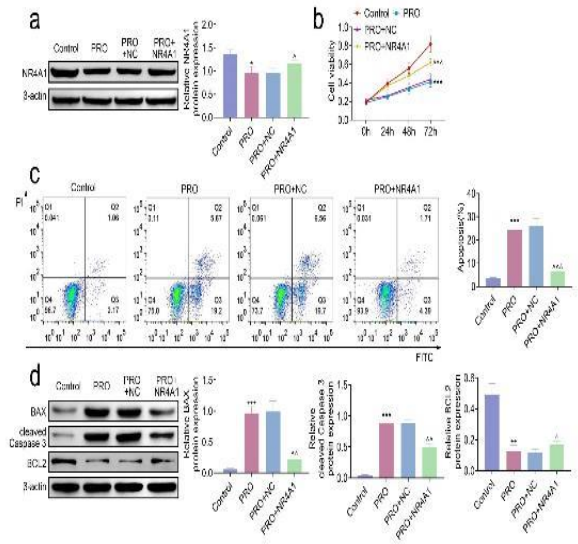

Figure 3: NR4A1 regulated cell motility in PRO-induced NSCs. NR4A1 was transfected into NSCs. (A): The expression of NR4A1 was detected by RT-qPCR; (B): Cell viability was detected by MTT assay; (C): Apoptosis and; (D): apoptosis-related protein expression was detected by flow cytometry and western blotting. * shows the PRO group compared with the control group; *$p < 0.05$; **$p < 0.01$; ***$p < 0.001$. ^PRO + NR4A1 group compared with PRO + NC group; ^$p < 0.05$; ^^$p < 0.01$; ^^^$p < 0.001$

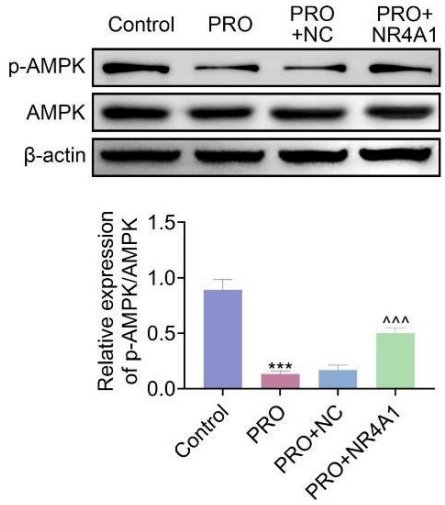

Figure 4: NR4A1 activates the AMPK pathway. AMPK pathway-related protein expression was determined by western blotting. *PRO group compared with the control group; ***$p < 0.001$; ^PRO + NR4A1 group compared with PRO + NC group; ^^^$p < 0.001$

DISCUSSION

The critical period for the development of brain learning and memory functions is from the end of pregnancy to the early postnatal period, when the nervous system is unusually sensitive to changes in the internal and external environment [10]. A study has shown that repeated and heavy use of propofol during this period leads to neurotoxicity in the developing brain, thus promoting apoptosis of the neuronal cells and impairment of their cognitive functions [11].

It has been claimed that the repeated use of PRO can cause an increased expression of c-fos and caspase-3, as well as an inducement of neuronal modulation, ultimately leading to cognitive impairment [11]. C-fos protein also plays a role in the initiation of apoptosis. Thus, PRO causes damage to neurons by promoting apoptosis. In addition, PRO inhibits long-duration enhancement by inhibiting AKT and extracellular regulatory protein kinase (ERK) signaling pathways. Long-term enhancement is an important mode of central nervous system plasticity, which forms the basis of the learning memory. The inhibition of long-range enhancement can lead to the impairment of cognitive functions in the brain. [12]. In the present study, the experimental results showed that PRO promoted apoptosis and inhibited cell viability and the activation of AMPK pathway in NSCs.

In order to explore the neurotoxic mechanism of PRO in-depth, the gene expression data of PRO samples and normal control samples were downloaded from GEO database, and the differentially expressed genes were successfully mined via GEO2R online analysis, while the PPI network of GEGs was constructed using STRING database.

Finally, a significantly down-regulated differential gene, NR4A1, was obtained. NR4A1, also known as Nur77 and TR3, is a highly homologous orphan nuclear receptor which belongs to the steroid/thyroid hormone receptor superfamily [13]. NR4A1, as an early response gene, can be induced by a variety of stimuli such as inflammatory regulators, growth factors, and neurotransmitters in a wide range of cell types and organs [13]. NR4A1 molecular conformation changes after receiving signal stimulation, and exerts transcriptional regulation through specific recognition, binding to the regulatory regions of target genes which are involved in cell proliferation and apoptosis, and regulated by various pathways such as protease degradation, phosphorylation, and protein interactions [14].

It has been shown that by activating NR4A1 expression, oxygen-glucose deprivation (OGD)-induced neuronal apoptosis can be restored, thus increasing neuronal survival and alleviating ischemia-induced injury [15]. Therefore, it was speculated that NR4A1 has a neuroprotective effect [15]. Furthermore, it has been reported that NR4A1 expression is decreased in young rats treated with propofol, and by analyzing the GEO database (GSE106799), it was found that NR4A1 expression was significantly decreased in the hippocampal region of young mice treated with propofol. Moreover, qRT-PCR and western blotting results also showed that NR4A1 expression was down-regulated in NSCs. Interestingly, this study found that the promotion of apoptosis and the inhibition of cell viability were both alleviated by NR4A1, indicating that it indeed has a neuroprotective effect.

NR4A1 activates the AMPK pathway, which is down-regulated in PRO-induced neural stem cell activity, and mitigates anesthetic damage to nerve cells by activating AMPK [16]. AMPK is an energy sensor that regulates inflammatory responses, oxidative stress and synaptic plasticity in acute and chronic brain injury [17,18]. In this study, NR4A1 reversed PRO-induced de-activation of the AMPK pathway, thus indicating that NR4A1 serves to protect nerves from PRO damage by modulating the pathway.

CONCLUSION

The most closely related hubgene, NR4A1, has been finally identified in this study. NR4A1 alleviates PRO-induced promotion of apoptosis and inhibition of cell viability by regulating AMPK pathway, which in turn alleviates the toxicity of propofol-induced neural stem cells in early life. There are, however, several other significantly down-regulated DEGs in PPI network, which need to be further verified via relevant experiments.

DECLARATIONS

Acknowledgements

None provided.

Funding

None provided.

Ethical approval

None provided.

Availability of data and materials

The datasets used and/or analyzed during the current study are available from the corresponding author on reasonable request.

Conflict of Interest

No conflict of interest associated with this work.

Contribution of Authors

We declare that this work was done by the authors named in this article and all liabilities pertaining to claims relating to the content of this article will be borne by the authors. Miaomiao Zhu and Jing Hu designed the study and carried them out; Miaomiao Zhu, Jing Hu, Baofeng Gao, Changlin Liu, Huiqing Li and Zengzhen Zhang supervised the data collection, analyzed the data, and interpreted the data; Miaomiao Zhu and Jing Hu prepared the manuscript for publication and reviewed the draft of the manuscript. All authors read and approved the manuscript for publication.

REFERENCES

1. *Jiang Y, Wang Y, Sun Y, Jiang H. Long non-coding RNA Peg13 attenuates the sevoflurane toxicity against neural stem cells by sponging microRNA-128-3p to preserve Sox13 expression. PLoS One 2020; 15(12): e0243644.*
2. *Shao LJ, Zou Y, Xue FS. Anesthesia-induced developmental neurotoxicity in children: past, present, and future. Chin Med J (Engl) 2019; 132(16): 1990-1992.*
3. *Schaefer ML, Wang M, Perez PJ, Coca Peralta W, Xu J, Johns RA. Nitric Oxide Donor Prevents Neonatal Isoflurane-induced Impairments in Synaptic Plasticity and Memory. Anesthesiology 2019; 130(2): 247-262.*
4. *Hausburg MA, Banton KL, Roman PE, Salgado F, Baek P, Waxman MJ, Tanner A, 2nd, Yoder J, Bar-Or D. Effects of propofol on ischemia-reperfusion and traumatic brain injury. J Crit Care 2020; 56(281-287.*
5. *Cao XZ, Ma H, Wang JK, Liu F, Wu BY, Tian AY, Wang LL, Tan WF. Postoperative cognitive deficits and neuroinflammation in the hippocampus triggered by surgical trauma are exacerbated in aged rats. Prog Neuropsychopharmacol Biol Psychiatry 2010; 34(8): 1426-1432.*
6. *He HJ, Wang Y, Le Y, Duan KM, Yan XB, Liao Q, Liao Y, Tong JB, Terrando N, Ouyang W. Surgery upregulates high mobility group box-1 and disrupts the blood-brain barrier causing cognitive dysfunction in aged rats. CNS Neurosci Ther 2012; 18(12): 994-1002.*
7. *Rockne RC, Adhikarla V, Tsaturyan L, Li Z, Masihi MB, Aboody KS, Barish ME, Gutova M. Long-term stability and computational analysis of migration patterns of L-MYC immortalized neural stem cells in the brain. PLoS One 2018; 13(8): e0199967.*
8. *Ren ZH, Wu K, Yang R, Liu ZQ, Cao W. Differential expression of matrix metalloproteinases and miRNAs in the metastasis of oral squamous cell carcinoma. BMC Oral Health 2020; 20(1): 24.*
9. *Yan F, Wufuer D, Ding J, Wang J. MicroRNA miR-146a-5p inhibits the inflammatory response and injury of airway epithelial cells via targeting TNF receptor-associated factor 6. Bioengineered 2021; 12(1): 1916-1926.*
10. *Ma D, Williamson P, Januszewski A, Nogaro MC, Hossain M, Ong LP, Shu Y, Franks NP, Maze M. Xenon mitigates isoflurane-induced neuronal apoptosis in the developing rodent brain. Anesthesiology 2007; 106(4): 746-753.*
11. *Cui Y, Ling-Shan G, Yi L, Xing-Qi W, Xue-Mei Z, Xiao-Xing Y. Repeated administration of propofol upregulated the expression of c-Fos and cleaved-caspase-3 proteins in the developing mouse brain. Indian J Pharmacol 2011; 43(6): 648-651.*
12. *Gao J, Peng S, Xiang S, Huang J, Chen P. Repeated exposure to propofol impairs spatial learning, inhibits LTP and reduces CaMKIIα in young rats. Neurosci Lett 2014; 560(62-66.*
13. *Jiang Q, Wang Y, Shi X. Propofol Inhibits Neurogenesis of Rat Neural Stem Cells by Upregulating MicroRNA-141-3p. Stem Cells Dev 2017; 26(3): 189-196.*
14. *Maruyama K, Tsukada T, Ohkura N, Bandoh S, Hosono T, Yamaguchi K. The NGFI-B subfamily of the nuclear receptor superfamily (review). Int J Oncol 1998; 12(6): 1237-1243.*
15. *Liu LL, Qiao S, Wang ML, Wu HK, Su YX, Wang KM, Liu XW. MiR224-5p Inhibitor Restrains Neuronal Apoptosis by Targeting NR4A1 in the Oxygen-Glucose Deprivation (OGD) Model. Front Neurosci 2020; 14(613.*
16. *Liang C, Du F, Wang J, Cang J, Xue Z. Propofol Regulates Neural Stem Cell Proliferation and Differentiation via Calmodulin-Dependent Protein Kinase II/AMPK/ATF5 Signaling Axis. Anesth Analg 2019; 129(2): 608-617.*
17. *Zhong H, Hao L, Li X, Wang C, Wu X. Anti-inflammatory role of trilobatin on lipopolysaccharide-induced acute lung injury through activation of ampk/gsk3β-nrf2 pathway. Signa Vitae 2020; 16(2): 160-166.*
18. *Wang J, Peng Z, Huang K, Yin J, Feng C, You T, Tan W. Isoglycyrrhizin protects mouse lungs against acute respiratory distress syndrome via regulation of AMPK/Nrf2/ARE pathway. Trop J Pharm Res 2021; 20(10): 2071-2076.*